

Study of deconfinement in NA50

PAULA BORDALO^{6,b} for the NA50 Collaboration

M C Abreu^{6,a}, B Alessandro¹⁰, C Alexa³, R Arnaldi¹⁰, M Atayan¹², C Baglin¹, A Baldit², M Bedjidian¹¹, S Beolè¹⁰, V Boldea³, Paula Bordalo^{6,b}, S R Borenstein^{9,c}, C Borges⁶, A Bussière¹, L Capelli¹¹, C Castagner², J Castor², B Chaurand⁹, B Cheynis¹¹, E Chiavassa¹⁰, C Cicalò⁴, T Claudino⁶, M P Comets⁸, N Constans⁹, S Constantinescu³, P Cortese^{10,d}, J Cruz⁶, A De Falco⁴, G Dellacasa^{10,d}, N De Marco¹⁰, A Devaux², S Dita³, O Drapier¹¹, B Espagnon², J Fargeix², P Force², M Gallio¹⁰, Y K Gavrilo⁷, C Gersche¹, P Giubellino¹⁰, M B Golubeva⁷, M Gonin⁹, A A Grigorian¹², J Y Grossiord¹¹, F F Guber⁷, A Guichard¹¹, H Gulkanyan¹², R Hakobyan¹², R Haroutunian¹¹, M Idzik^{10,d}, D Jouan⁸, T L Karavitcheva⁷, L Kluberg⁹, A B Kurepin⁷, Y Le Bornec⁸, C Lourenço⁵, P Macciotta⁴, M Mac Cormick⁸, A Marzari-Chiesa¹⁰, M Masera¹⁰, A Masoni⁴, M Monteno¹⁰, A Musso¹⁰, P Petiau⁹, A Piccotti¹⁰, J R Pizzi¹¹, W Prado Da Silva^{10,e}, F Prino¹⁰, G Puddu⁴, C Quintans⁶, S Ramos^{6,b}, L Ramello^{10,d}, P Rato Mendes⁶, L Riccati¹⁰, A Romana⁹, P Saturnini², H Santos⁶, E Scalas^{10,d}, E Scomparin¹⁰, S Serci⁴, R Shahoyan^{6,f}, F Sigaud¹⁰, S Silva⁶, M Sitta^{10,d}, P Sonderegger^{5,b}, X Tarrago⁸, N S Topilskaya⁷, G L Usai⁴, E Vercellin¹⁰, L Villatte⁸ and N Willis⁸

¹LAPP, CNRS-IN2P3, Annecy-le-Vieux, France

²LPC, Univ. Blaise Pascal and CNRS-IN2P3, Aubière, France

³IFA, Bucharest, Romania

⁴Università di Cagliari/INFN, Cagliari, Italy

⁵CERN, Geneva, Switzerland

⁶LIP, Lisbon, Portugal

⁷INR, Moscow, Russia

⁸IPN, Univ. de Paris-Sud and CNRS-IN2P3, Orsay, France

⁹LPNHE, Ecole Polytechnique and CNRS-IN2P3, Palaiseau, France

¹⁰Università di Torino/INFN, Torino, Italy

¹¹IPN, Univ. Claude Bernard Lyon-I and CNRS-IN2P3, Villeurbanne, France

¹²YerPhI, Yerevan, Armenia

^aAlso at FCT, Universidade de Algarve, Faro, Portugal

^bAlso at IST, Universidade Técnica de Lisboa, Lisbon, Portugal

^cOn leave of absence from York College CUNY

^dUniversità del Piemonte Orientale, Alessandria and INFN-Torino, Italy

^eNow at UERJ, Rio de Janeiro, Brazil

^fOn leave of absence of YerPhI, Yerevan, Armenia

Abstract. The J/ψ production in 158 A GeV Pb–Pb interactions is studied, in the dimuon decay channel, as a function of centrality, as measured with the electromagnetic or, alternatively, with the very forward hadronic calorimeters. After a first sharp variation at mid-centrality, both patterns continue to fall down and exhibit a curvature change at high centrality values. This trend excludes any conventional hadronic model and finds a natural explanation in a deconfined quark–gluon phase scenario.

Paula Bordalo

Keywords. J/ψ anomalous suppression; quark–gluon plasma; deconfinement.

PACS Nos 25.75.-q; 25.75.Nq; 13.20.Gd; 14.40.Gx

1. Introduction

A phase transition from ordinary hadronic matter to a new state of deconfined quarks and gluons is predicted by non-perturbative quantum chromodynamics (QCD) [1] under extreme conditions which could be reached in reactions induced by ultrarelativistic heavy ion beams as available at the CERN-SPS.

NA50 is a dimuon experiment searching for specific signals of deconfinement, namely the suppression of charmonia production which is considered a probe of quark–gluon plasma (QGP) formation in the earliest stage. Indeed, it has been predicted [2] that the $c\bar{c}$ bound states are prevented to be formed by the colour screening potential in the very dense medium undergoing a phase transition to a deconfined medium of quarks and gluons. Among the $c\bar{c}$ bound states, J/ψ is particularly interesting because it is highly tied and so it cannot be easily broken by interactions in a dense hadronic medium.

The NA50 recent observations of an anomalous J/ψ suppression [3], a threshold effect [4] and a double stepwise suppression pattern [5] are strong indications of the deconfinement transition.

In this presentation, previously published conclusions find further support both with new results based on proton-induced interactions which lead to a more precise measurement of J/ψ normal absorption and with different analyses of the same Pb–Pb data which either use directly minimum bias events for normalization or estimate the centrality of the collision from the forward hadronic energy measured in the very forward hadronic calorimeter.

2. Experimental setup and data selection

The NA50 apparatus [6] mainly consists of a muon spectrometer, a segmented active target and three independent centrality detectors: an electromagnetic calorimeter which measures the neutral transverse energy (E_T) produced in the interaction, a zero degree calorimeter (E_{ZDC}) measuring the very forward hadronic energy of the spectator nucleons and a silicon strip multiplicity detector of charged particles.

In this analysis we use data taken in 1996 and 1998 with a lead beam impinging on a Pb target, as well as the new proton–nucleus data of 1998–2000 ($A \equiv \text{Be, Cu, Al, Ag, W, Pb}$) taken at two different beam intensities together with previous measurements with the same dimuon spectrometer of other light systems: sulphur–uranium results from NA38 [10] and proton–proton and proton–deuterium measured by NA51 [7].

The kinematical domain used for dimuon detection, $2.92 \leq y_{\text{lab}} \leq 3.92$ (i.e., $0 \leq y_{\text{cms}} \leq 1$, for Pb–Pb at 158 GeV/n) and $|\cos \theta_{\text{CS}}| < 0.5$ leads, in the mass region of interest, to acceptances of the order of 15%. The centrality detectors cover the following pseudorapidity domains: electromagnetic calorimeter, $1.1 < \eta_{\text{lab}} < 2.3$; zero degree calorimeter, $\eta_{\text{lab}} > 6.3$; multiplicity detector, $1.1 < \eta_{\text{lab}} < 4.18$.

Study of deconfinement in NA50

The J/ψ is detected via its decay into muon pairs. Combinatorial background, due to π and K decays, is estimated from like-sign pairs [6], using $N_{BG} = 2\sqrt{N^2+N^{2-}}$. The muon pairs selected for the analyses satisfy the standard NA50 criteria [3].

Pb–Pb data taking conditions were similar in all the periods reported here, except for the total thickness of the target and the number of individual sub-targets. The segmented lead target was made, in 1996, of seven sub-targets with a total thickness of 12 mm corresponding to 30% of an interaction length. In order to eliminate events with possible unidentified re-interactions which could contaminate Pb–Pb central collisions, its total thickness was reduced to 3 mm (7% λ_I) in 1998, leaving only one single Pb sub-target. As a consequence and for this 1998 sample of data, peripheral Pb–Pb collisions were not studied due to the the relative high contamination originating from Pb–air interactions. In order to avoid the interactions of Pb ions with air, we have run last year with the target placed in vacuum; the analysis of these data is underway and the results will be available soon.

A contour-cut selection (based on the correlation $E_T - E_{ZDC}$) [3] which is satisfied by interactions originating from the target region was systematically applied to the data samples. The result of the selection is shown in figure 1 for the two Pb–Pb data sets. Moreover, when studying the E_T dependence of J/ψ production, sub-target identification by the target instrumentation was further required for the analysis which makes use of the muonless, and therefore more loosely constrained, minimum bias events.

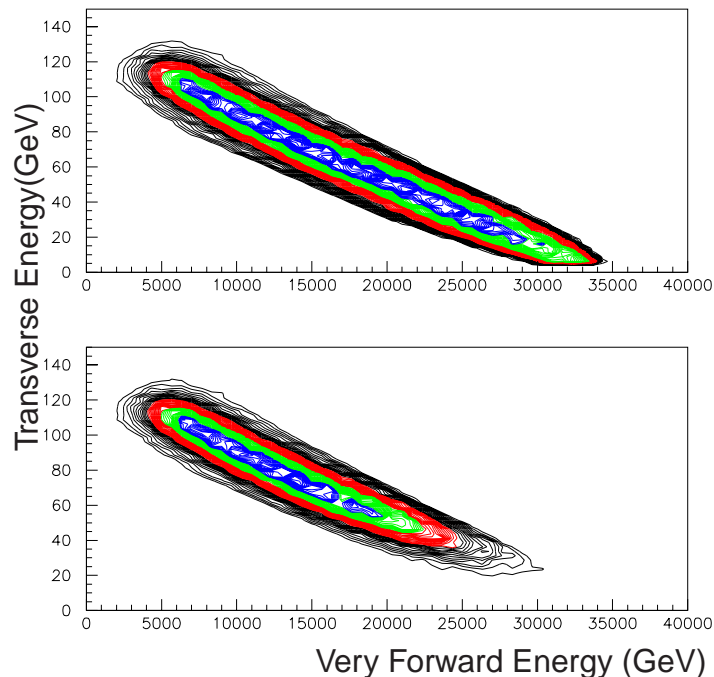


Figure 1. The correlation between transverse neutral energy and very forward energy for selected events of 1996 (above) and 1998 (below) data.

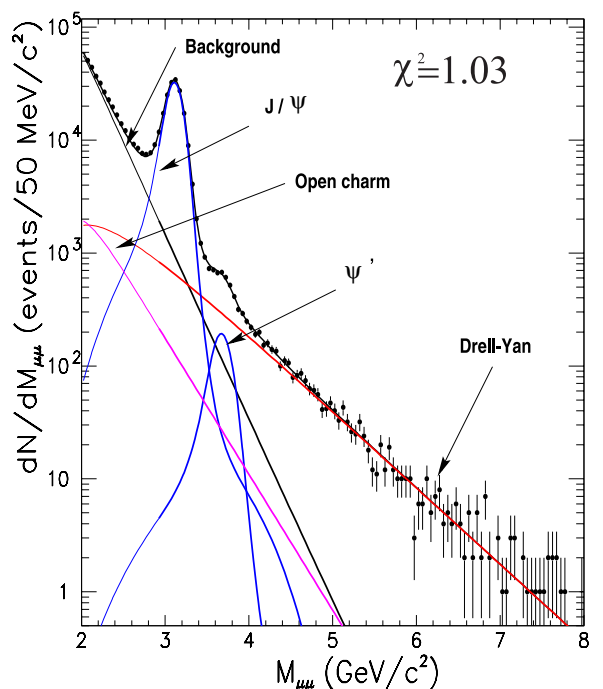


Figure 2. Opposite sign muon pair invariant mass spectrum for Pb–Pb collisions at 158 GeV/nucleon.

3. Fit procedure

Various physical processes account for the raw opposite sign muon pair invariant mass spectrum shown in figure 2.

Besides J/ψ and ψ' resonances and the Drell–Yan mechanism, the mass continuum includes contributions from the combinatorial background and from muon pairs originating from semi-leptonic decays of charmed mesons (mainly open charm ($D\bar{D}$) production). The combinatorial background is mainly due to uncorrelated π and K decays into muons. It is computed from the like-sign mass distributions using $dN/dM|^{bkg} = 2R\sqrt{\frac{dN^2}{dM} + \frac{dN^2}{dM}}$, where R accounts for the effects of charge correlations. Its proper value has been determined as described in ref. [8].

The opposite sign muon pair invariant mass distribution is fitted according to the following procedure in order to determine the amount of its different components. The shapes of the muon pairs originating from J/ψ and ψ' decays and from the Drell–Yan process are obtained from a simulation of the NA50 detector using the same reconstruction and selection criteria as used for the real data.

Each kind of events, J/ψ , ψ' , Drell–Yan and $D\bar{D}$, is simulated and reconstructed with the NA50 program used for analysis of the real data. The Drell–Yan contribution is calculated at the leading order and uses the MRSA structure functions, which takes into account the \bar{u}/\bar{d} asymmetry as measured by the NA51 experiment [7]. The $D\bar{D}$ shape is taken from

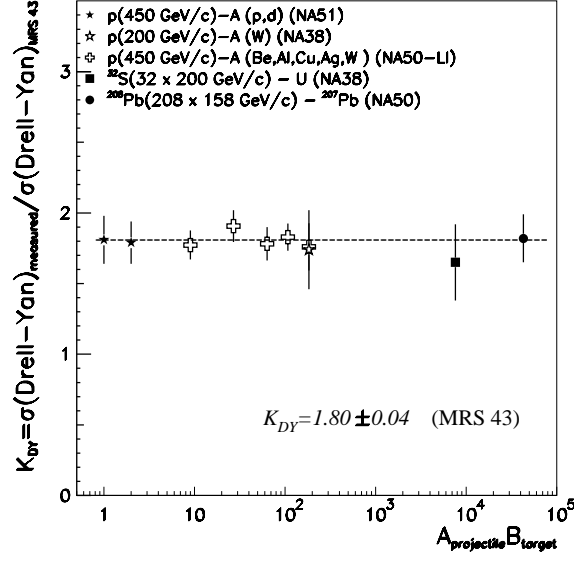


Figure 3. Drell–Yan K -factor as a function of $A_{\text{proj}} \cdot B_{\text{tgt}}$.

a Pythia simulation including the resolution of the NA50 detector. A charm-like excess [8] is allowed on its normalization.

Finally, the amplitudes of J/ψ , ψ' and Drell–Yan contributions are obtained from a fit to the experimental data for $M_{\mu\mu} > 2.9 \text{ GeV}/c^2$ according to

$$\frac{dN}{dM} = A_{J/\psi} \frac{dN_{J/\psi}}{dM} + A_{\psi'} \frac{dN_{\psi'}}{dM} + A_{\text{DY}} \frac{dN_{\text{DY}}}{dM} + \frac{dN_{D\bar{D}}}{dM} + \frac{dN_{BG}}{dM}.$$

The detailed description of the analysis method is reported in [6].

4. J/ψ production as a function of E_T

4.1 The ratio of J/ψ over DY

A systematic study of Drell–Yan behaviour, ranging from p – p and some p – A systems to S – U and Pb – Pb is shown in figure 3 which displays the ratio between the measured and computed Drell–Yan cross-sections, the so-called K -factor, as a function of the product of the projectile and target atomic mass numbers $A \cdot B$. Its constant value proves that DY cross-section behaves normally and is proportional to the number of elementary nucleon–nucleon collisions. So, it is used as a reference in the study of J/ψ production.

The J/ψ cross-section per nucleon–nucleon collision can thus be studied from the ratio of the J/ψ to Drell–Yan cross-sections. This ratio is almost free from systematic errors, which are identical in both samples (only 1.5% left) and cancel out in the ratio.

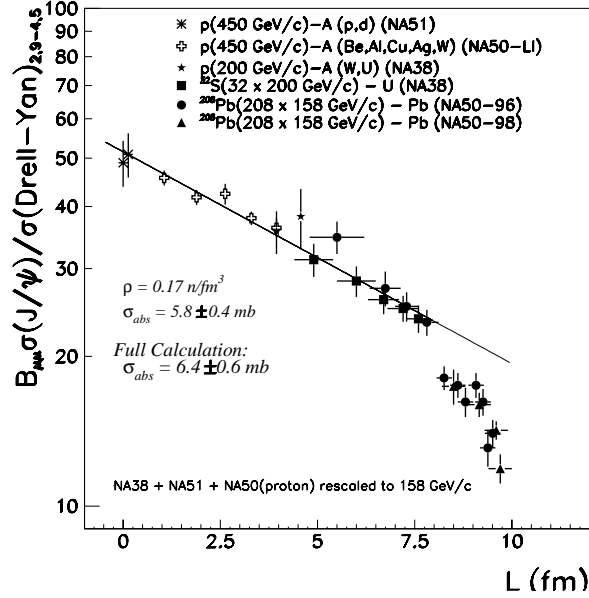


Figure 4. $J/\psi/DY$ as a function of L . The absorption curve is a fit to p - A and S - U experimental data.

Figure 4 shows the ratio for a large number interacting systems (from p - p and several p - A to S - U and Pb - Pb), as a function L , the path length that the pre-resonant $c\bar{c}g$ state has to go through in nuclear matter (which allows a common description of the different systems) [3].

A simple exponential parametrization applied to the lighter systems (NA38 [9–11] and NA51 [7] data ranging from p - p to S - U together with the new NA50 p - A data), namely assuming $B_{\mu\mu}\sigma^{\psi}/\sigma^{DY} \propto e^{-\rho L\sigma_{abs}}$, gives an absorption cross-section of the $c\bar{c}g$ state in nuclear matter of $\sigma_{abs} = 5.8 \pm 0.4$ mb. The full Glauber calculation lead to an absorption cross-section of the J/ψ in the ordinary hadronic matter of $\sigma_{abs} = 6.4 \pm 0.6$ mb). This experimental value of J/ψ nuclear σ_{abs} measured with the same dimuon spectrometer as that used in Pb - Pb collisions sets the baseline for the J/ψ production pattern obtained in Pb - Pb interactions.

Whereas the more peripheral Pb - Pb points lie on the absorption curve, the more central ones show a sudden 20% drop at $L \simeq 8$ fm, suggesting the onset of another J/ψ suppression mechanism.

The ratio of J/ψ to Drell-Yan cross-sections has also been studied as a function of E_T , for the various Pb - Pb data taking periods, using two different methods as described below.

In the first method (standard analysis), the Drell-Yan and J/ψ yields are obtained from the standard fit procedure described above. The results are displayed in figure 5. An agreement among all Pb - Pb data is seen, except for the most central point of 1996 which is affected by reinteractions on its thicker target (12 mm) as reported in [5]. A sudden drop around 40 GeV followed by a continuous decrease is observed.

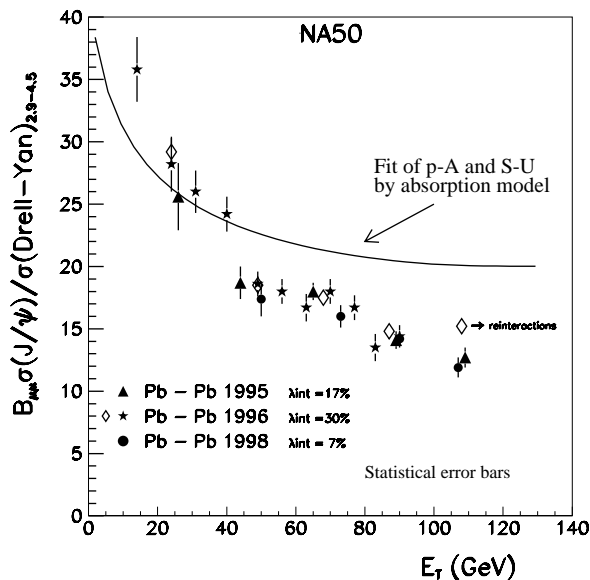


Figure 5. $J/\psi/DY$ as a function of E_T . The absorption curve is a fit to p - A and S - U experimental data.

In the second method, which does not use any fit, the J/ψ yield is obtained from a simple counting method without any fitting procedure and the Drell-Yan is deduced from the large minimum bias (MB) sample of events (thus reducing significantly statistical errors but introducing another sources of systematic errors). This is obtained by multiplying the experimental E_T spectrum of the MB events by the ratio of the fitted experimental E_T spectra of DY and MB with the Glauber model. For a detailed description of the procedure, see [4].

As shown in figure 6, the two methods lead to very similar results in the domain where re-interactions are negligible. Only statistical error bars are displayed.

The same figure also displays the results based on the 1998 data analyzed with the minimum bias method, which agree with the 1996 analyses while exploring higher E_T values without reinteraction contamination. The solid line presented in the figure corresponds to the ordinary nuclear absorption obtained from the study of lighter systems data (from p - p to S - U) which lead to $\sigma_{\text{abs}} = 6.4$ mb. The overall displayed distribution exhibits, besides a 20% drop at 40 GeV (corresponding to $L \simeq 8$ fm), an inflexion point around 90 GeV followed by a steady steep decrease.

In order to put together in the same picture all data samples (p - p , p - A , S - U and Pb - Pb collisions) collected with the same dimuon spectrometer (NA51, NA38 and NA50 experiments), we calculate as a function of the energy density ε the ratio between the observed J/ψ yield and the expected by the nuclear absorption curve which reproduces the measurement of our lighter systems, from p - p to S - U . The results are presented in figure 7 and the same two-step J/ψ pattern suppression is observed.

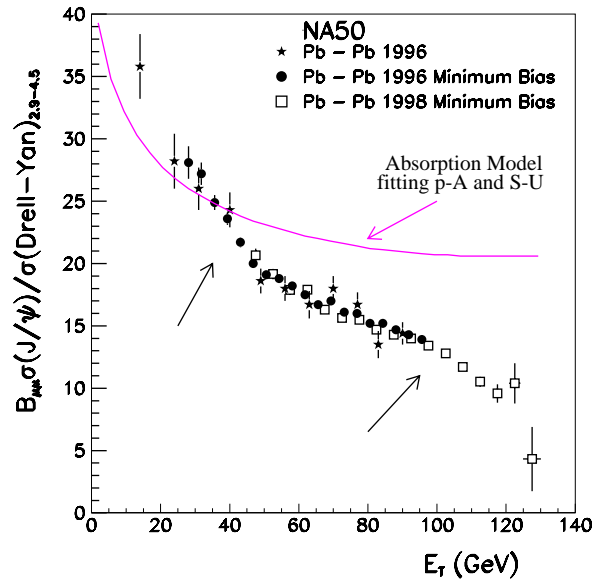


Figure 6. $J/\psi/DY$ as a function of E_T .

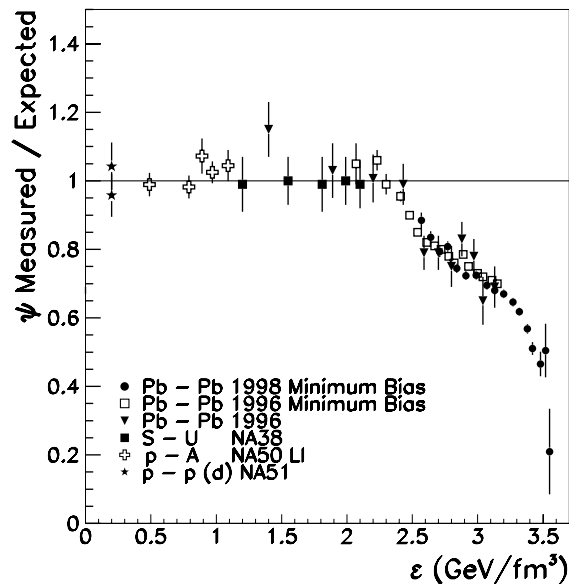


Figure 7. J/ψ measured/expected by our absorption model as a function of the energy density ϵ .

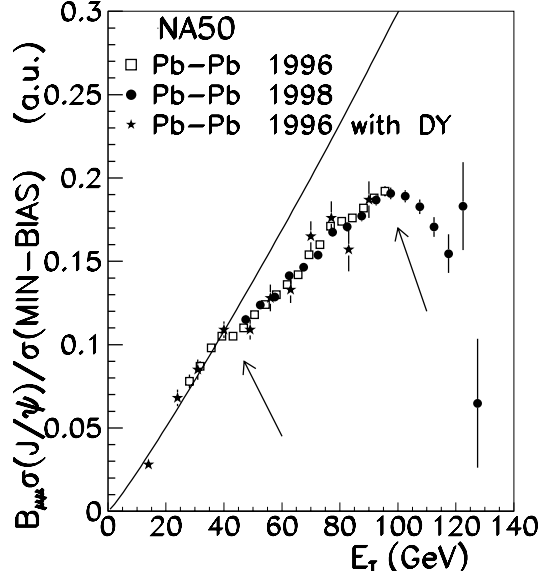


Figure 8. J/ψ /minimum bias as a function of E_T . The curve stands for our absorption model as measured with light systems.

4.2 The ratio of J/ψ to minimum bias cross-sections

We report the ratio of the J/ψ to minimum bias cross-sections as a function of E_T . As shown in figure 8, a clear departure from the absorption model, quoted above, is observed at $E_T \simeq 40$ GeV whereas at E_T around 90 GeV a change of behaviour is seen. Both observations are in agreement with the J/ψ /DY analysis, reinforcing the J/ψ anomalous suppression picture.

5. The E_{ZDC} dependence of J/ψ production

Results of an independent analysis of J/ψ /DY using the forward energy E_{ZDC} measured in a zero-degree calorimeter (ZDC) as an estimator of centrality are displayed in figure 9 for the two data sets analyzed with the minimum bias method.

Once again two clear changes of the J/ψ suppression slope are observed: a sudden drop at $E_{ZDC} \simeq 26$ TeV (corresponding to the impact parameter $b \simeq 8$ fm) and a steady decrease for the most central collisions at $E_{ZDC} \simeq 9$ TeV.

6. Discussion of the results

Different theoretical models based on conventional assumptions [12–16] or in a quark–gluon plasma phase transition [17,18] have been developed and compared to the NA50 observations.

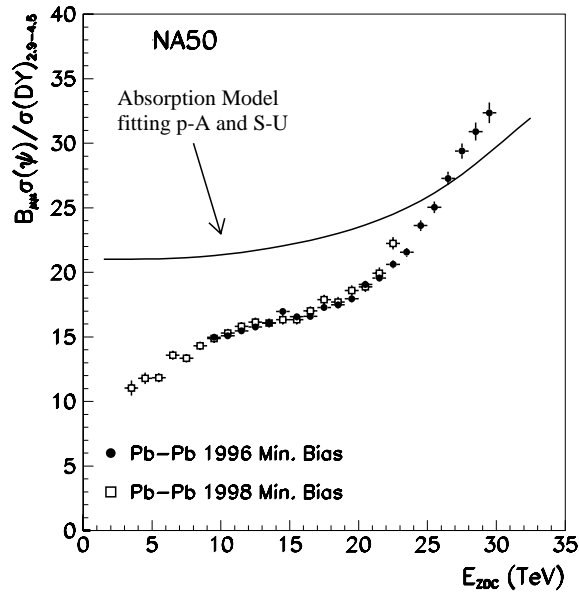


Figure 9. $J/\psi/DY$ as a function of E_{ZDC} using the minimum bias method.

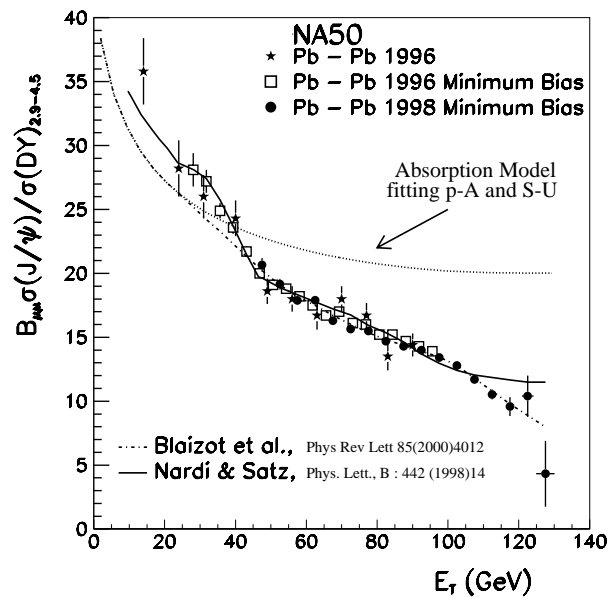


Figure 10. $J/\psi/DY$ minimum bias as a function of E_T compared with two models within quark-gluon plasma framework.

Study of deconfinement in NA50

None of the conventional models can describe simultaneously both the $J/\psi/DY$ results measured with proton and sulphur induced reactions and the pattern of $J/\psi/DY$ as a function of E_T obtained in Pb–Pb collisions.

Models including quark–gluon deconfinement with two thresholds, corresponding respectively to the χ_c and the J/ψ melting points [17] together with E_T fluctuations [18] are qualitatively in much better agreement with the experimental observations as shown in figure 10.

Recently, with the development of QCD calculations in the lattice [19], new approximative models [20,21] have the possibility of charmonia states (namely the χ_c) dissociation, at a temperature T_d in hot nuclear matter, before deconfinement at the critical temperature T_c . For the J/ψ $c\bar{c}$ state it is not clear if T_d is greater or lesser than T_c . Before drawing final conclusions one needs a complete calculation and that the predictions be given as a function of measured variables.

7. Conclusions

New data and analyses give further support to the published results on Pb–Pb reactions by experiment NA50 which show a stepwise J/ψ anomalous suppression pattern. While J/ψ production agrees with normal nuclear absorption for the most peripheral Pb–Pb reactions, a departure of about 20% from this normal behaviour occurs for semi-peripheral collisions and is followed, with increasing centrality, by an inflexion point and a steady steep decrease for the most central reactions. This pattern can be interpreted as due to the successive melting of charmonium bound states (χ_c , J/ψ) as predicted by quark–gluon deconfinement, or to the dissociation of the χ_c in the hadronic matter and the melting of J/ψ in deconfined matter. The anomalous J/ψ pattern suppression observed in NA50 experiment is a clear evidence of the transition to a deconfined state of matter.

Acknowledgements

This work was partially supported by Fundação para a Ciência e a Tecnologia, by INTAS grant 96-0231 and by the Russian Foundation for Fundamental Research, grant 99-02-16003.

References

- [1] C Bernard *et al*, *Phys. Rev. Lett.* **D54**, 4586 (1996)
- [2] T Matsui and H Satz, *Phys. Lett.* **B178**, 416 (1986)
- [3] M C Abreu *et al*, (NA50 Coll.), *Phys. Lett.* **B410**, 337 (1997)
- [4] M C Abreu *et al*, (NA50 Coll.), *Phys. Lett.* **B450**, 456 (1999)
- [5] M C Abreu *et al*, (NA50 Coll.), *Phys. Lett.* **B477**, 28 (2000)
- [6] M C Abreu *et al*, (NA50 Coll.), *Phys. Lett.* **B410**, 327 (1997)
- [7] M C Abreu *et al*, (NA51 Coll.), *Phys. Lett.* **B438**, 35 (1998)
- [8] M C Abreu *et al*, (NA38 and NA50 Coll.), *Euro. Phys. J.* **C14**, 443 (2000)
- [9] M C Abreu *et al*, (NA38 Coll.), *Phys. Lett.* **B444**, 516 (1998)
- [10] M C Abreu *et al*, (NA38 Coll.), *Phys. Lett.* **B449**, 128 (1999)

Paula Bordalo

- [11] M C Abreu *et al*, (NA38 Coll.), *Phys. Lett.* **B466**, 408 (1999)
- [12] J Geiss *et al*, *Phys. Lett.* **B117**, 31 (1999)
- [13] C Spieles *et al*, *Phys. Rev.* **C60**, 54901 (1999)
- [14] D E Kahana *et al*, *Prog. Part. Nucl. Phys.* **42**, 269 (1999)
- [15] N Armesto *et al*, *Phys. Rev.* **C59**, 395 (1999)
- [16] A Capella *et al*, *Phys. Rev. Lett.* **85**, 2080 (2000)
- [17] M Nardi and H Satz, *Phys. Lett.* **B442**, 14(1998)
- [18] J P Blaizot *et al*, *Phys. Rev. Lett.* **85**, 4012 (2000)
- [19] F Karsch *et al*, *Nucl. Phys.* **B605**, 579 (2001)
- [20] S Digal *et al*, *Phys. Lett.* **B514**, 57 (2001)
- [21] C Y Wong *et al*, *Phys. Rev.* **C65**, 34902 (2002)